







Figure 4 shows the experimental setup to investigate wavelength conversion by double-pass cSHG/DFG with the different phase control schemes. A tuneable external cavity laser (ECL) was used as fundamental source; a fixed wavelength distributed feedback laser (DFB) served as signal source. Polarization controlled (PC) signal and fundamental waves were combined by a 3 dB coupler and boosted by an erbium doped fiber amplifier (EDFA). The light was butt coupled to the temperature stabilized double-pass waveguide. The wavelength conversion spectra were recorded in backward direction using a circulator and an optical spectrum analyzer (OSA).

In addition, due to the small transmittance of the end face mirror(s), also single-pass wavelength conversion spectra could be measured in forward direction.

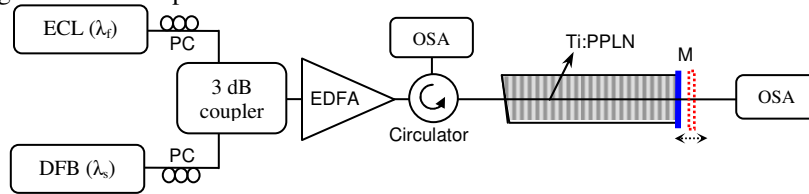


Fig. 4. Experimental setup to investigate double-pass cSHG/DFG: ECL - external cavity laser; DFB - distributed feedback laser; PC - fiber optical polarization controller; EDFA - erbium doped fiber amplifier; OSA - optical spectrum analyser; M - dielectric mirrors, deposited on waveguide end face and movable, respectively.

### 3.1 Phase control with dichroic mirrors of adjustable spacing

Phase control can be achieved by reflecting the different waves with two sequential dichroic mirrors: The first one, which is directly deposited on the polished waveguide end face, was designed to highly reflect the SH wave ( $\sim 98\%$ ) and to transmit only  $\sim 2\%$  of the fundamental, signal, and idler waves (Fig. 5, blue graph). The second mirror is an external one and its separation from the first one can be adjusted; it is a broadband high reflector of more than 98% reflectance for fundamental, signal, and idler waves but of high transmittance for the SH-wave (Fig. 5, red graph).

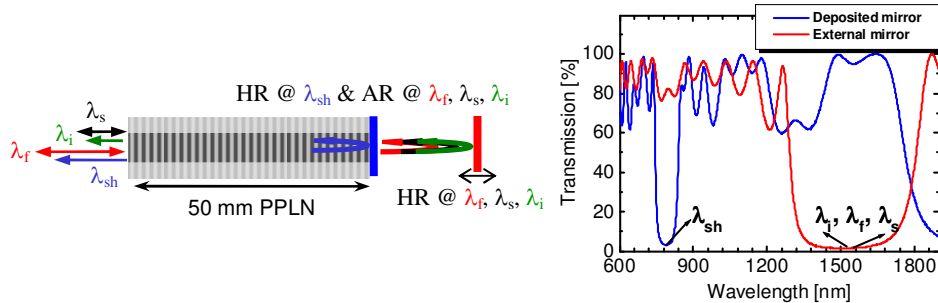


Fig. 5. Left: Double pass-configuration using two dichroic mirrors. AR - anti reflection coated; HR - high reflection coated. Right: Measured transmission versus wavelength of the mirror deposited on the waveguide end face (blue) and of the external moveable mirror (red).

By controlling the separation  $\Delta z$  of the external mirror to the waveguide end face within half a fundamental wavelength, the phase relationship between the reflected SH wave and the fundamental, signal, and idler waves can be adjusted by  $\Delta\phi_{\text{comp}} = 2\pi(2\Delta z)/\lambda_f$ , leading to maximum power transfer from the fundamental to SH, signal, and idler waves. As long as the mirror separation  $\Delta z$  is smaller than a wavelength, the coupling loss back into the waveguide is negligible; therefore,  $\Delta z < 1 \mu\text{m}$  was adjusted.

Using this scheme an improvement of cSHG/DFG-based wavelength conversion of 7.5 dB has been achieved in comparison to the single-pass configuration for the same device of 50

mm length. In Fig. 6 the experimental results for SHG (left diagram) together with the cSHG/DFG wavelength conversion spectra (right diagram) are shown. The improvement of 7.5 dB agrees reasonably well with the theoretically predicted 10 dB for an effective interaction length of 35 mm derived from the single-pass SHG characteristics.

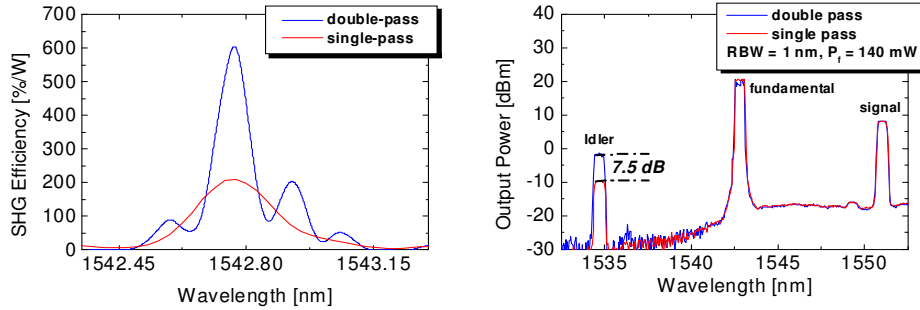


Fig. 6. Left: Measured single- and double-pass SHG efficiency versus fundamental wavelength. Right: Measured spectra for single- and double-pass wavelength conversion by cSHG/DFG. Device temperature was 190 °C in both experiments.

### 3.2 Exploiting the dispersion of LiNbO<sub>3</sub> within an unpoled waveguide section

In this case the waveguide is not completely periodically poled but has an unpoled section L just in front of the broadband dielectric mirror; it reflects both, fundamental and SH wavelength ranges (Fig. 7, right).

#### 3.2.1 Higher order approach, allowing wavelength tuning

If the unpoled waveguide section has a length of several mm (Fig. 7, left), the phase relation between the interacting waves can be easily changed within  $2\pi$  by slightly tuning the fundamental wavelength within the acceptance bandwidth of the QPM-condition (0.3 nm in our device for the single-pass).

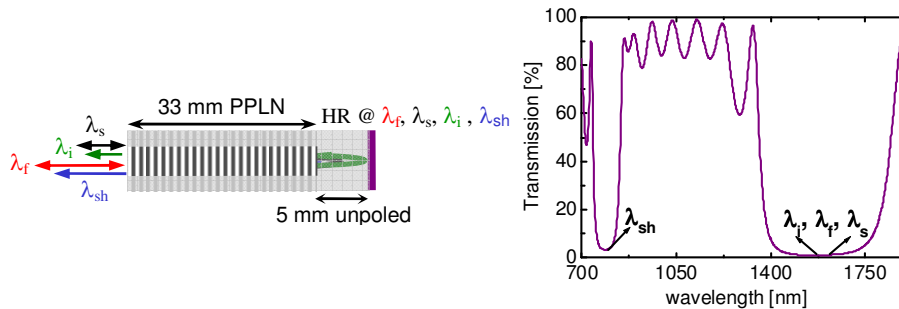


Fig. 7. Left: Operating scheme for higher order approach. Right: Measured transmission of the broadband dielectric mirror deposited on the polished waveguide end face.

In the 5 mm long unpoled waveguide section used in our experiments, a total relative phase change due to dispersion  $\Delta\phi_{\text{dispersion}} = \Delta\phi_{\text{dispersion, sh}} - 2\Delta\phi_{\text{dispersion, f}} = 2(2\pi/\lambda_f)(2L)(n_{\text{sh}} - n_f)$  of about  $1000(2\pi)$  is induced. It strongly depends on the fundamental wavelength yielding a slope of  $d(\Delta\phi_{\text{dispersion}})/d(\lambda_f) \approx 10\pi/\text{nm}$ . Therefore, a very small tuning of the fundamental wave is sufficient to adjust phase compensation. In our experiment a wavelength change of only 29 pm resulted in a 5 dB improvement of the double-pass SHG efficiency compared to the single-pass result (Fig. 8, left). This was the basis to get nearly 9 dB improvement of signal to idler conversion efficiency for cSHG/DFG-based wavelength conversion (Fig. 8, right).

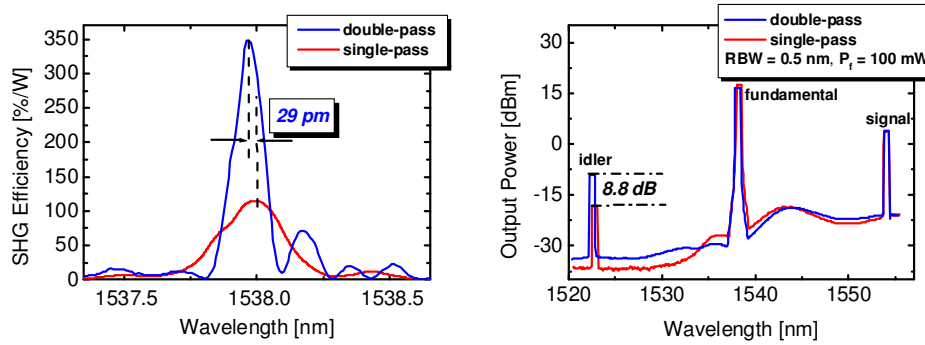


Fig. 8. Left: Measured single- and double-pass SHG efficiencies versus the fundamental wavelength. Right: Measured spectra for single- and double-pass wavelength conversion by cSHG/DFG. Device temperature was 190 °C in both experiments.

### 3.2.2 Zero order approach, selecting the right section length

The same adjustment can be achieved by a very short waveguide section of appropriate length, corresponding to a fraction of half a domain period ( $\Lambda/2 = L_c$ ). Waveguide sections of slightly different lengths before the end face mirror were fabricated by tilting a homogeneous domain grating over a set of waveguides. Then the specific channel leading to optimum phase compensation with  $\Delta\varphi_{\text{comp}} = 2\pi L/L_c$  can be selected.

The operating scheme to investigate double-pass cSHG/DFG-based wavelength conversion in the zero order approach is shown in Fig. 9, left. A slightly tilted ( $< 1^\circ$ ), homogeneous domain grating across the waveguides leads to different fractions of the final domain period in front of the mirror. The dependence of the SHG-efficiency on the length of this last domain fraction has been investigated (Fig. 9, right). The results confirm the strong phase dependence of the double-pass efficiency and allow selecting the optimum waveguide.

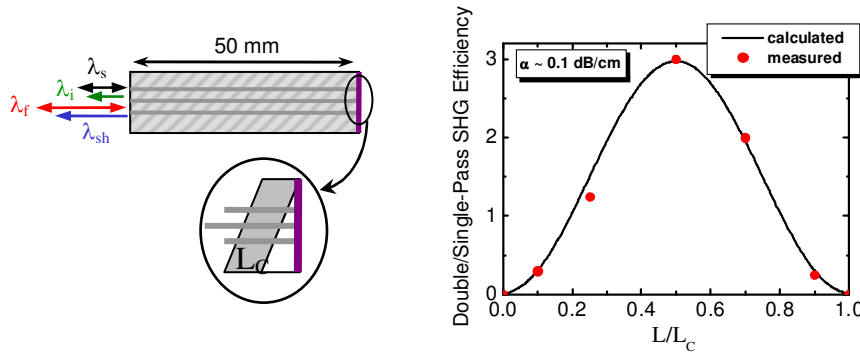


Fig. 9. Left: Schematic drawing of the Ti:PPLN-waveguide sample with a tilted domain grating ( $L$  indicates the wedged domain fraction,  $L_c$  is the width of a complete domain). Right: Measured and calculated double-pass SHG efficiency with respect to the single-pass efficiency for waveguides with different fractions  $L/L_c$  of the last domain, propagation loss  $\alpha \sim 0.1$  dB/cm.

Using this specific waveguide, SHG-efficiency and cSHG/DFG-based wavelength conversion have been investigated for both, single- and double-pass configuration, respectively. The results are shown in Fig. 10. On the left, the SHG characteristics are plotted; besides a spectral narrowing, an improvement of the efficiency of about 5 dB was achieved in comparison with the single-pass result, similar to the higher order approach. On the right, cSHG/DFG-based wavelength conversion spectra are shown; the conversion efficiency could

be improved by 8.5 dB. As this compensation scheme is of zero order ( $\Delta\phi_{\text{comp}} < 2\pi$ ), a large bandwidth can be expected suitable for multi-wavelength conversion in WDM-systems.

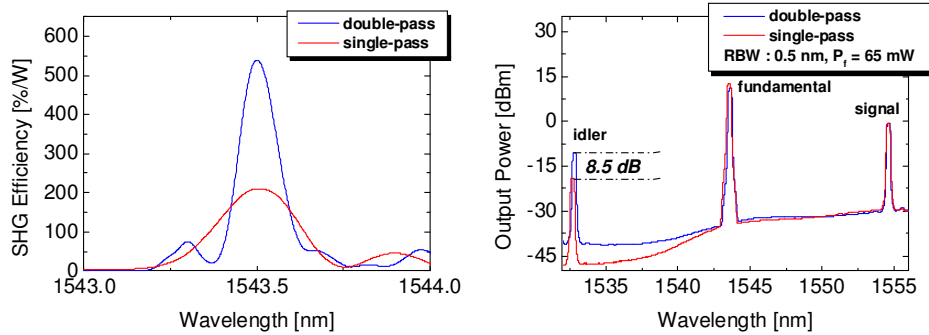


Fig. 10. Left: Measured single- and double-pass SHG-efficiencies versus the fundamental wavelength. Right: Measured spectra for single- and double-pass wavelength conversion by cSHG/DFG. Device temperature was 190 °C in both experiments.

The difference of the noise levels for single- and double-pass conversion in the vicinity of the idler wavelength is due to the different conversion efficiencies for the amplified spontaneous emission (ASE) of the EDFA in front of the waveguide (see Fig. 4). This difference becomes visible if the power level of the converted ASE is larger than the power level of the unconverted ASE in the same wavelength range. The optical signal to noise ratio (OSNR) could be improved by suppressing the ASE in front of the waveguide by appropriate filtering.

#### 4. Conclusions

SHG and cSHG/DFG-based wavelength conversion in the C-band of optical communications have been investigated using Ti:PPLN waveguides in single- and double-pass configuration, respectively. To optimize the wavelength conversion efficiency in the double-pass device three different schemes for compensating wavelength dependent phase shifts by reflection have been investigated. The most promising one is compensation by dispersion in a short ( $< \Lambda/2$ ) waveguide section, enabling even broadband operation. Using this scheme, the SHG-efficiency could be improved by 5 dB compared to the single-pass approach. The efficiency for wavelength conversion in the C-band by cSHG/DFG was improved by even 8.5 dB close to the theoretical limit of 10 dB (assuming an effective interaction length of 35 mm).

#### Acknowledgment

This work has been funded by the Deutsche Forschungsgemeinschaft (DFG) within the project “Contention Resolution in Optical Burst Switching (OBS) using Wavelength Conversion.”